

Int. J. Electrochem. Sci., 12 (2017) 3050 – 3062, doi: 10.20964/2017.04.60

International Journal of
**ELECTROCHEMICAL
SCIENCE**

www.electrochemsci.org

An investigation of Digoxin by Cyclic Voltammetry using Gold and Silver Solid Electrodes and Chemometric Analysis

G. F. Bellia, H. Corrall, M. G. Baron, R. Croxton, J. Gonzalez-Rodriguez*

School of Chemistry, College of Science, University of Lincoln, Brayford Pool, Lincoln, LN67TS, UK. Telephone: +441522886878.

*E-mail: jgonzalezrodriguez@lincoln.ac.uk

Received: 24 January 2017 / *Accepted:* 28 February 2017 / *Published:* 12 March 2017

Digoxin, one of the main cardiac glycosides medication, has shown to have a strong analytical response under investigation by voltammetric analysis using mercury electrodes, achieving nanomole sensitivity. In this study we investigated the suitability of solid electrodes as gold and silver electrodes in voltammetric analysis of this active pharmaceutical ingredient. The scope of the investigation was to evaluate if the use of these solid electrodes, more practical and especially less dangerous, under an operative and environmental aspects could represent a valid further possibility to add to the use of the mercury ones. Both of the solid electrodes have been tested at different pH of 5, 7.4, 10, and 11. PCA analysis has been performed and specific responses achieved. Micromole sensitivity has been achieved for both of the electrodes, showing that the use of these sensors could represent a preliminary analytical approach when the more accurate alternative choice is not necessary, being more practical and less environmental impacting than using mercury.

Keywords: digoxin, voltammetry, solid electrodes, PCA analysis

1. INTRODUCTION

Digoxin (Figure 1) is a cardiac glycoside obtained from Lanatoside C, a matrix glycoside present mainly in the leaves and seeds of *Digitalis purpurea* (commonly known as Foxglove) [1]. It is used for the treatment of congestive heart failure, a condition in which the heart is unable to pump blood efficiently around the body [2]. This, in turn, can cause fluid to collect in the lungs and body tissues and lead to congestion. Digoxin is utilised to solve this as it is believed to inhibit Na⁺-K⁺ ATPase in addition to activating contractile elements of muscle fibres [2]. It increases the cellular calcium uptake in cardiac cells and enhances Na⁺-Ca²⁺ exchange. Digoxin acts as a stimulant on the cardiac muscles as well as on un-striated and skeletal muscles, renal tubules and stray nerve centres.

Determination of the concentration of digoxin in blood, the heart and the kidney is, therefore, vital in order to confirm poisoning from ingestion of this compound. Digoxin has a double interest as a clinical molecule but also as a potential poison that could lead to heart failure [3].

The therapeutic action of digoxin starts around two hours after oral administration and 15–30 min after intravenous administration. The half-life period of digoxin via these methods is 1.5–2 days. Digoxin concentration in blood should be tested in order to find the appropriate dose for the given individual. However, digoxin has only a small therapeutic range of concentrations (0.5–2.0 ng/mL)[1] and because of this index, digoxin therapy requires strict monitoring of blood levels in order to minimize toxicity [2-5].

Digoxin concentrations in vitro or in blood and urine samples have been determined previously using many techniques such as SEM [1, 6]; HPLC (with and without pulsed amperometric detection) [7-13]; LC-MS [14-18]; voltammetry [19,20], chemiluminescence immunoassay [21] and reverse-phase thin-layer chromatography [22]. Digoxin tablets have been analysed using laser-induced fluorescence polarization [23].

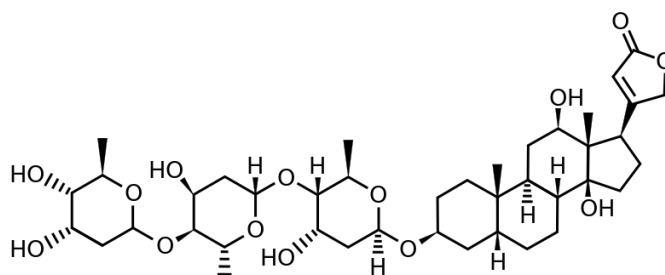


Figure 1. Chemical structure of digoxin.

Examples of the use of electrochemical methods using solid electrodes for the determination of drugs in clinical [29, 30] or forensic applications [31-35] is not novel. Due to the selectivity and sensitivity achieved by the electrochemical techniques it is becoming more and more popular for their applications in sensors or sensing elements.

Digoxin has been extensively studied using adsorptive stripping voltammetry by Wang et al. [19], where mercury electrodes were analysed by differential-pulse voltammetric analysis. The use of this technique allows a sensitivity of nanomole order. However, the hanging mercury drop electrode can present some shortcomings due to the inner mechanisms required to produce the drop. When using the hanging mercury drop technique the size of the drops has to be reproducible and remain unchanged to guarantee accurate and reproducible results. In order to achieve this, a mercury flow from the Hg reservoir to the tip of the electrode is stopped at selected time intervals to produce a static as opposed to a growing drop. There are many factors that can lead to an unstable drop size. Firstly, during the filling of the mercury reservoirs, small bubbles of air can become trapped. Even a small bubble of air can cause serious interferences with the stability of the drop.

Secondly, regulation of the pressure applied to the drop at the end of each analysis has to be accurately set up. It is important that the pressure is high enough to continuously replace the drop but not too high that the drop becomes stressed during the scan and its size changes.

Environmental issues, due to the toxicity of Hg, must be taken into account as well. Although mercury can be regenerated and reused, disposal of this element poses danger to the operator as well as large costs for disposal treatments. Solid metal electrodes, on the other hand, have no such environmental implications and provide an accurate polishing phase at the end of each analysis, which guarantees a constant analytical surface and in turn ensures reproducibility of results. Despite the excellent cathodic potential range of mercury, its anodic range is severely limited with respect to main solid metal electrodes due to its ability to oxidise easily. Solid electrodes also have the potential to be used in portable analytical devices.

Solid metal electrodes, such as silver and gold, have not been previously reported being used in any voltammetric studies to analyse digoxin.

The aim of this study, therefore, is to investigate the use of gold and silver electrodes to analyse digoxin and compare the results with those found in the literature, obtained from Hg electrode.

2. EXPERIMENTAL

Digoxin (CAS No.: 20830-75-5, IUPAC name 3-[(3S,5R,8R,9S,10S,12R,13S,14S,17R)-3-[(2R,4S,5S,6R)-5-[(2S,4S,5S,6R)-5-[(2S,4S,5S,6R)-4,5-dihydroxy-6-methyloxan-2-yl]oxy-4-hydroxy-6-methyloxan-2-yl]oxy-4-hydroxy-6-methyloxan-2-yl]oxy-12,14-dihydroxy-10,13-dimethyl-1,2,3,4,5,6,7,8,9,11,12,15,16,17-tetradecahydrocyclopenta[a]phenanthren-17-yl]-2H-furan-5-one, Alumina (Aluminum oxide Al_2O_3 , CAS No.: 1344-28-1, 150 mesh) and Silica (Silicon dioxide amorphous CAS No.: 112945-52-5, fumed, particle size 0.007 μm) were obtained from Sigma Aldrich, UK. Methanol, (CH_3OH , CAS No.: 67-56-1) was obtained from Fischer Scientific, UK. Sodium Acetate Trihydrate ($\text{CH}_3\text{COONa}\cdot 3\text{H}_2\text{O}$, CAS No.: 6131-90-4), Sodium Hydroxide (NaOH , CAS No.: 1310-73-2), Sodium phosphate dibasic dodecahydrate ($\text{Na}_2\text{HPO}_4\cdot 12\text{H}_2\text{O}$, CAS No.: 10039-32-4), Sodium phosphate monobasic dihydrate ($\text{NaH}_2\text{PO}_4\cdot 2\text{H}_2\text{O}$, CAS No.: 13472-35-0), Sodium Carbonate (Na_2CO_3 , CAS No.: 497-19-8) and Sodium hydrogen carbonate (NaHCO_3 , CAS No.: 144-55-8) were obtained from Fischer International, UK. Glacial Acetic Acid (CH_3COOH , CAS No.: 64-19-7) was obtained from BDH Acids HP, USA. Gold and silver electrodes were obtained from Metrohm, UK.

Digoxin stock solutions were prepared by dissolving digoxin in methanol at a range of concentrations of 200 $\mu\text{g}/\text{mL}$. The solutions were stored in the dark at 4 $^\circ\text{C}$.

The pH5 buffer was prepared using glacial acetic acid (0.2M) and $\text{CH}_3\text{COONa}\cdot 3\text{H}_2\text{O}$ (0.2M) at a ratio of 30:70 v/v. The pH=7.4 buffer was prepared using $\text{Na}_2\text{HPO}_4\cdot 12\text{H}_2\text{O}$ (0.2M) and $\text{NaH}_2\text{PO}_4\cdot 2\text{H}_2\text{O}$ (0.2M) at a ratio of 81:19 v/v. The pH=10 buffer was prepared using Na_2CO_3 (0.1M) and NaHCO_3 (0.1M) at a ratio of 60:40 v/v. The pH=11 buffer was prepared using NaOH (0.005M) solution (Fischer International, UK).

Cyclic voltammograms were obtained using a 757 VA Computrace Metrohm connected to a Compaq deskpro personal computer. The reference electrode was Ag/AgCl (KCl 3M). The working

solid gold and silver working electrodes also acted as stirrer. Platinum electrodes were used as auxiliary electrode.

Before each new analysis and after the last of the set, each electrode was cleaned in order to remove traces of any electro-active substances that may be present.

First, the electrode was removed from the apparatus and washed under a flow of deionised water. Next, a single drop of deionised water and a spatula tip sized amount of alumina was then mixed in a petri dish to make a paste. The tip of the electrode was then cleaned in this paste by making 10 circular rotations in each direction, three times, as well as a ten figure of 8 movements in each direction, three times. The top of the electrode was then washed under a flow of deionised water before finally being sonicated in deionised water for 3 minutes.

To perform cyclic voltammetry analyses, 10ml of a selected buffer solution was poured into the measuring cell with an aliquot of digoxin stock solution to reach varying concentrations from 3.9- 14.8 $\mu\text{g/ml}$. The resulting solutions were deoxygenated by a flow of nitrogen for 5 minutes. No accumulation potential was applied. 3 cyclic voltammetry scans were performed on each buffer solution, with a RED-OX potential range of +2V to -2V. The sweep rate was kept at 0.05 V/s and the voltage step at 0.0059 V. All data was obtained at 25°C.

Principal Component Analysis (PCA) was performed using Tanagra data mining software (University of Lyon, France). Voltammogram data was exported from the voltammetry apparatus to an excel spreadsheet and subsequently uploaded onto Tanagra.

Medusa graph analysis software (Royal Institute of Technology, Stockholm, Sweden) has been used to analyse and visualize the concentration of the different species in solution vs pH.

3. RESULTS AND DISCUSSION

Digoxin was used in a comparison study of the electrochemical interactions of gold and silver solid metal electrodes in different pH buffer solutions using cyclic voltammetry. A good comprehension of the features of the different electrodes under different pH conditions was key to understand the electrochemical behaviour of digoxin and its interaction with the different metal surfaces.

3.1 Gold electrode

First, the gold electrode in a buffer solution (digoxin-free) was investigated in an oxidation-reduction scan cycle to explore the extent of its ability to oxidise and then return to its original state via a reduction process.

Figure 2 shows the oxidation of gold at different pHs from oxidation to reduction sweep. In an acidic condition, such as that of pH=5, the gold electrode does not present a visible peak in the oxidation

direction and presents a slight peak in the reduction direction. Pasta, Mantia and Cui [24] suggest a probable reaction for the oxidation of gold to be:

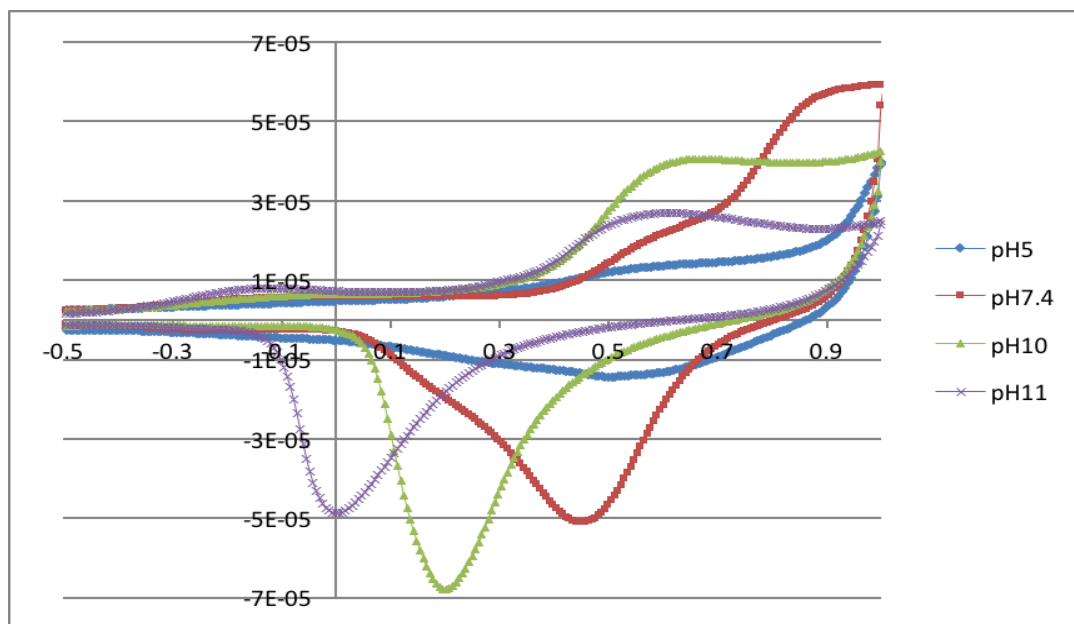


Figure 2. Voltammogram obtained using a gold electrode as a working electrode and different buffer solutions at different pHs of 5, 7.4, 10 and 11. Scan direction from -0.5V to +1V. Sweep rate = 0.05 V/s; Voltage step = 0.0059 V; T= 25°C.

A reaction such as this would be driven by alkaline pHs because the H^+ and OH^- ions may come together in solution, in turn driving the equilibrium of the reaction towards the formation of oxidised Au. It can be noted that as the pH of the buffer solution moves from acidic to alkaline the reduction peak shifts towards the negative potential, whereas the oxidation peak remains more or less constant at a potential of between +0.6V. The cathodic shift from right to left as the pH becomes increasingly alkaline can be explained by the consideration that the basic pH seems to favour the stability of the oxidised gold, which explains the higher voltage gap for the reduction current peak at the higher pH's [24]. This is in line with Kirk, Foulkes and Graydon [25] which reported the electrochemical formation of monolayers of Au(I) hydroxide in basic conditions close to pH=11.

Figure 3, obtained from Medusa software, shows the theoretical concentration of the different forms of oxidised Au as a function of pH at a fixed potential of 0.5V and a metal concentration of 10 μM to simulate an equilibrium process using thermodynamic criteria.

As the pH increases up to pH=9, a constant amount of gold is precipitating out of the solution and the concentration of H^+ ions is steadily decreasing. From pH5, the concentration of OH^- ions steadily increases.

$$E_H = 0.50 \text{ V}$$

$$[Au^+]_{TOT} = 10.00 \mu\text{M}$$

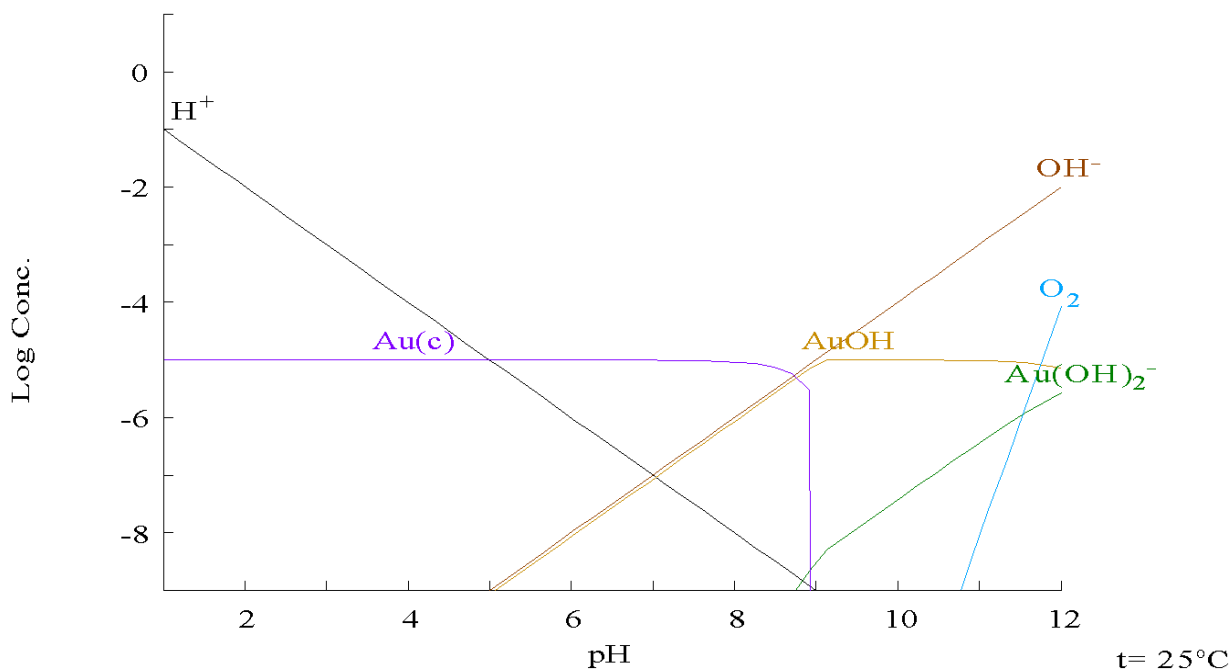


Figure 3. Theoretical oxidation-reduction equilibria for Au at 25°C and 10μM Au at different pHs.

Across pH=7, the level of H⁺ and OH⁻ ions are at equilibrium, which is to be expected as at a neutral pH the concentration of H⁺ and OH⁻ ions should be consistent. It can be noted that at pH9, the concentration of gold decreases dramatically, demonstrating the sudden conversion of gold to Au(OH)₂ ions. It is possible to identify (Figure 2) the formation of broad peaks in both reductive and oxidative scans, due to the chemisorption of hydroxide ions to the gold surface, in line with the report from Kirk et al [25]. At pH=5 Figure 3 also shows oxidation of gold from its metallic state to AuOH. This supports the results obtained from the cyclic voltammetry (Figure 2) for which an increase on surface oxides were obtained with an increase in pH. Similar results were reported both by Pasta, Mantia and Cui [24] who visualised the different oxidised species of Au at different potentials as a function of pH in the form of a Pourbaix diagram and by Nicol [36] who shown as gold at pH=7-12 is oxidized to Au(III) hydroxides, confirming the shift of the potentials shows in Figure 2.

Furthermore, the gold electrode was investigated in a reduction-oxidation scan cycle to discover the ability of the gold electrode to reduce and then revert back to its original state via oxidation. Similarly to the results observed in the oxidation-reduction scan, reduction peaks dependent on the pH of the oxidised gold are observed. The peak voltages decrease from 0.5V to 0V as the pH increases towards the alkaline region from pH=7.4 to pH=11. The oxidation reaction on the reduction sweep appears at the same range of voltages as those uncovered in the oxidation-reduction cycle. All of these factors demonstrated that the reactions on the surface of a gold electrode are fully reversible as expected.

3.2 Silver Electrode

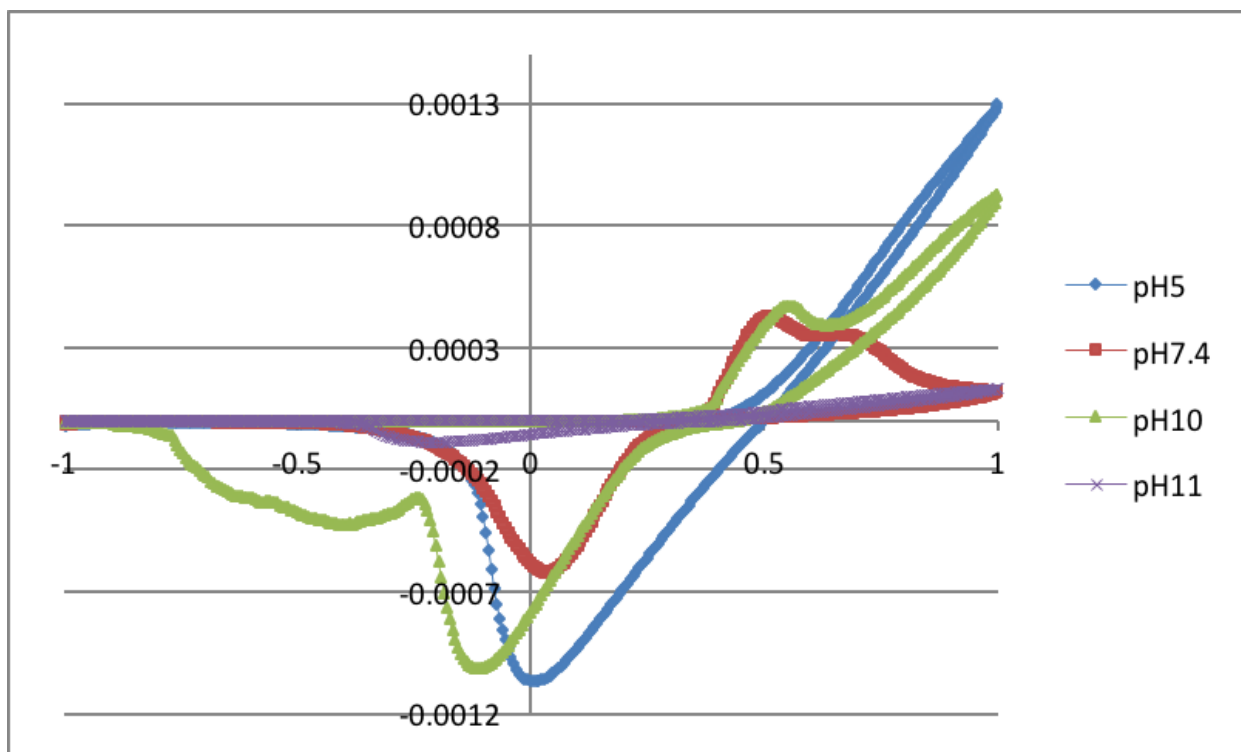


Figure 4. Voltammogram obtained using a silver electrode as a working electrode and different buffer solutions at different pHs of 5, 7.4, 10 and 11. Scan from -1V to +1V. Sweep rate = 0.05 V/s; Voltage step = 0.0059 V; T= 25°C.

Similarly to the investigation carried out for the gold electrode, the silver electrode was studied in an oxidation-reduction scan cycle first to discover the extent of its ability to oxidise and then reduce (Figure 4).

In the oxidation-reduction cycle where the silver electrode was employed, there is no evidence of an oxidation signal during the positive sweep in the acidic environment of pH=5. At the remaining pH levels of 7.4, 10 and 11, however, anodic peaks can be observed, in agreement with the results shown by Hassan et al [26]. When the scan is then reversed to reduce the products of the initial oxidation, only a weak signal was detected (-0.239V) in the alkaline conditions of pH11. The pH regions of 7.4 and 10 registered strong cathodic peaks.

Following this, the silver electrode was then studied by a reduction-oxidation scan cycle (Figure 5). In the reduction sweep of the silver electrode two peaks are visible at pH=7.4 (0.012V and -0.149V) and pH=10 (-0.3905V and -0.04745V) and only one at pH 5 (0 V).

When the scan then moves into the oxidation phase, sweeping towards the more positive potential, two peaks are present at pH=7.4, however at pH=10 only one oxidation peak is observed. No oxidation peaks were detected at pHs 5 and 11.

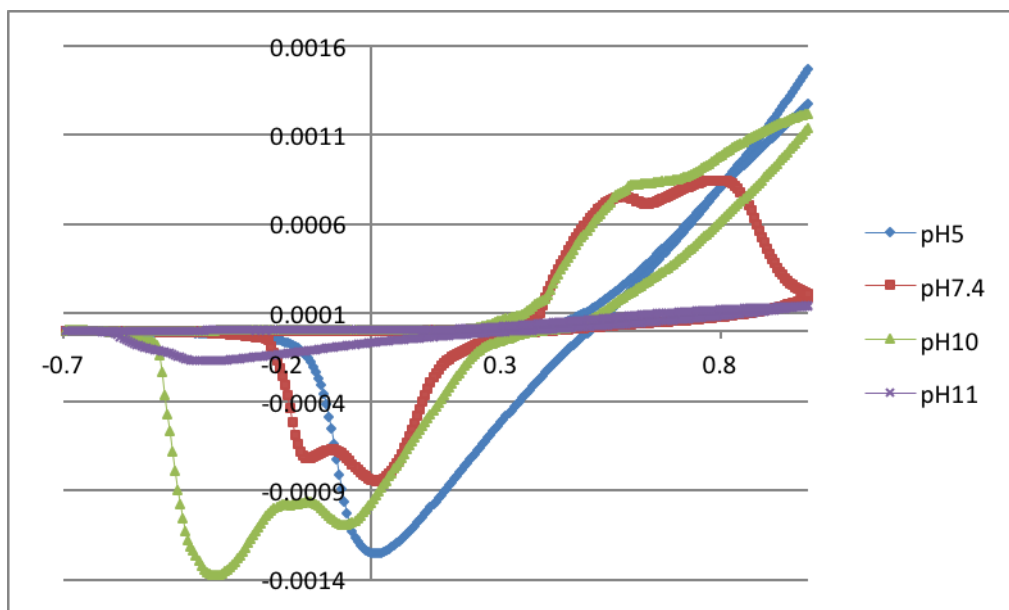


Figure 5. Silver electrode voltammogram in a reduction-oxidation scan cycle at different pHs of 5, 7.4, 10 and 11. Scan from +2V to -2V. Sweep rate = 0.05 V/s; Voltage step = 0.0059 V; T= 25°C.

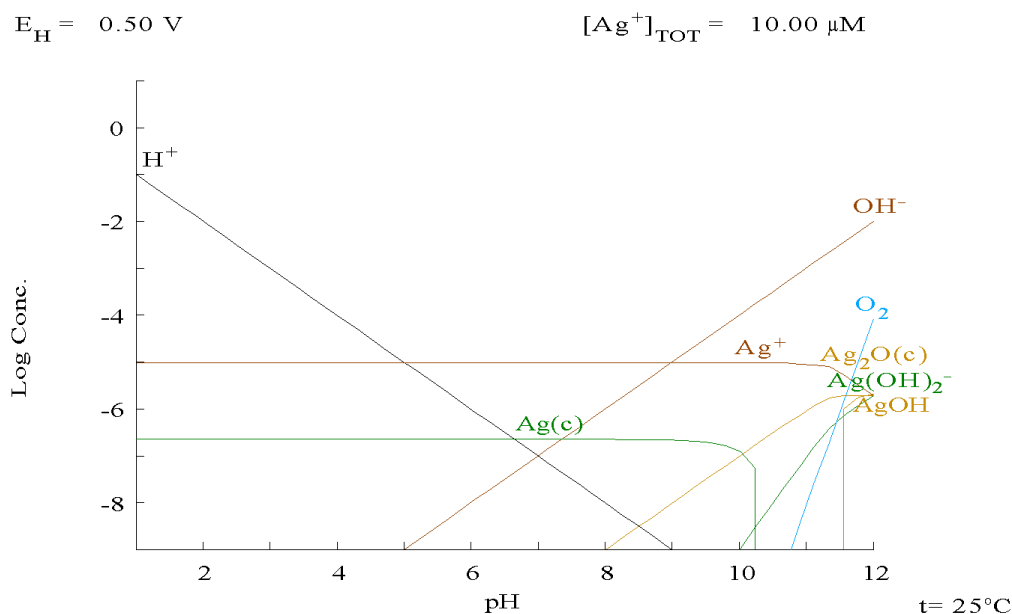


Figure 6. Theoretical oxidation-reduction equilibria for Ag at 25°C and 10µM Au at different pHs.

Figure 6 shows the concentration of the different forms of oxidised silver as a function of the pH at a fixed potential of 0.5V and silver concentration of 10µM. As the pH increases up to pH10, a constant amount of silver is precipitating out of solution and the concentration of H⁺ ions steadily decreases (expected as the pH is moving towards the alkaline condition). At the time that this is happening, up to pH11, a constant amount of Ag⁺ ions are forming. It can be noted that at pH8 Ag₂O also starts to precipitate out of solution. The concentration of both these ions begins to plateau at around pH11. From pH10 a sudden increase of Ag(OH)₂⁻ ions can be seen, followed by an appearance

of AgOH ions between pH=11 and 12. The presence of all of these ions at the differing pHs visually demonstrates the cyclic voltammetry results and the presence of surface oxides on the electrode, as well as supporting those results presented by Pasta, Mantia and Cui in the form of a Pourbaix diagram [24] and [26]. It is clear, from the evidence supplied here, that an important factor to consider when digoxin is to be added to a solution and analysed by an electrode system is the presence of metal oxides. Digoxin will have to compete with the electrode in both the oxidation and reduction processes occurring during cyclic voltammetry. This leads to a reduction in signal as the concentration of digoxin increases. There is a definite evidence of a linear dependence between the signal obtained and digoxin concentration.

3.3 Electrochemistry of digoxin under gold electrodes

By observing the chemical structure of digoxin, successful reduction and oxidation of the compound would be expected due to the presence of electroactive groups. As suggested by Ivanovskaya [20], the double bond conjugated to the carbonyl group of the molecule can be prone to reduction from an alkene to an alkane group, as well as oxidation as a result of the lactone ring being opened.

When using a gold electrode, at pH=5 and pH=7.4, an analytical peak during the reduction process at -1.21 and -1.27V, can be respectively seen, producing linear calibration curves with correlation coefficients of $r^2=0.9568$ and 0.9072 , respectively.

At pH=10, the gold electrode also showed a good analytical signal in the reduction phase at 0.23V, producing a linear regression of $r^2=0.976$. This electrode showed the best linearity of data ($r^2=0.9948$) at pH=11. At this pH, the gold electrode showed to be able to analyse digoxin in a reliable manner. It was possible to use two different points of the curve, at 0.601V in the anodic sweep and at 0.041V in the cathodic sweep respectively to build the calibration curve (with $R^2=0.9948$).

For the gold electrode the limit of detection (LoD) ranged from 55 $\mu\text{g/ml}$ at pH=5 to 1.7 $\mu\text{g/ml}$ at pH=11. The optimum pH for analysis was chosen to be pH=11.

This could be explained with the better response of the conversion of the equilibrium of the oxidised Au in alkaline medium as discussed earlier. This is also corroborated by lower values of the standard deviations at pH=11.

The average Coefficient of Variation also followed this trend showing a higher precision of 2.07% and 4.13% for both the anodic and cathodic peaks respectively at pH=11.

Principal Component Analyses of the different digoxin solutions were also performed, as shown in Figure 7. This PCA analysis of the results showed how the data obtained are well grouped in isolated clusters, especially the ones obtained at pH=11 where the points are closer to each other. The different clusters were helpful to discriminate the best pH conditions under any concentration, even blanks, to show any trends or surface behaviour and potential interactions. It is clear from the results achieved that pH is a key variable to determine the chemical reactions occurring on the surface of the electrode. Even the absence (blanks) or presence of digoxin in solution at different concentrations seems to be a secondary factor in the clustering as demonstrated by the fact that all voltammograms

clustered together. Different pHs will affect the position of the reduction and oxidation peaks and, as seen before, the reproducibility of these processes. Hence, to select the best possible analytical conditions for the analysis of digoxin on a gold electrode this is a factor that needs to be considered. The presence of surface oxides will greatly condition the electrochemical response. However, this is not a factor that prevents the analytical use of this electrode in the determination of digoxin as demonstrated by the calibration curves. The variability achieved in the analysis of each of the PCA plots was given by the percentage of variability for the different PCs. In this way for figure 7 and figure 8 this was PC1(53.79%) and PC2(26.86%) and PC1(51.30%) and PC2(29.94%), respectively.

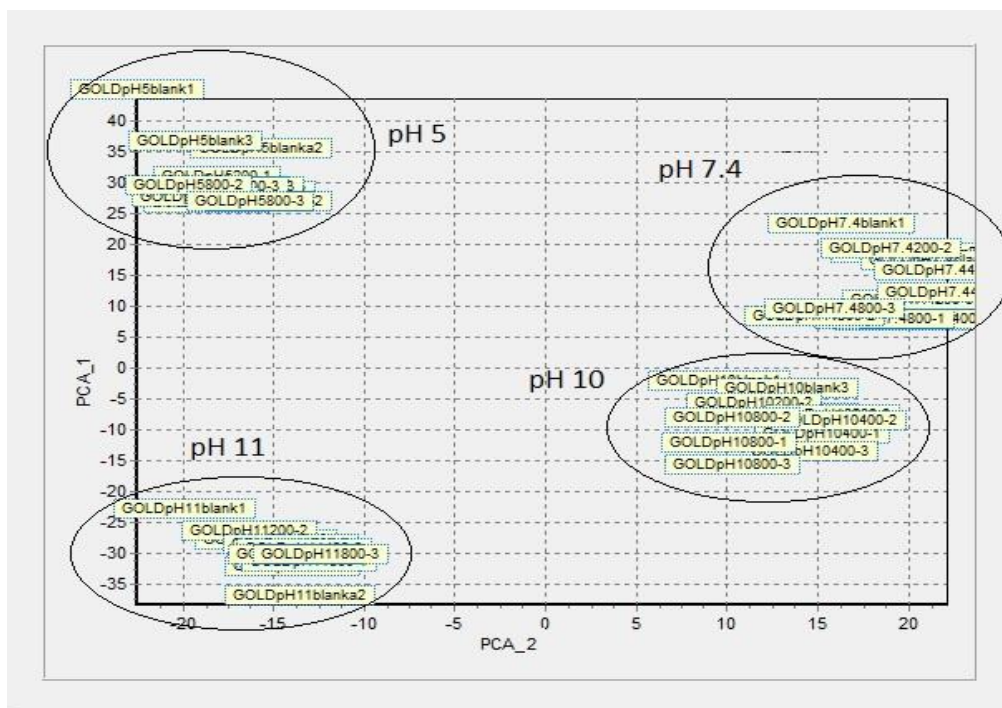


Figure 7. PCA scatterplot of the electrochemistry of a gold electrode at different pHs of 5, 7.4, 10, 11. Percentage of variability: PC1=53.79%; PC2=26.86%.

3.4 Electrochemistry of digoxin under silver electrodes.

Digoxin solutions at pH=5 showed the possibility to be also analysed using silver electrodes yielding peaks at 0.0055V and 0.0121V (in the reduction phase), showing calibration curves with $r^2=0.9269$ and 0.9874 , respectively. Solutions at pH=7.4 showed a non-ideal environment for the analytical use of silver electrodes as they were not able to detect digoxin in neither the cycles possibly due to the lack of interaction with surface oxides. At pH=10, silver electrodes could analyse digoxin at -0.12V during the reduction phase, achieving a calibration curve with a $R^2=0.9104$.

At pH=11, silver electrodes were able to detect digoxin obtaining calibration curves with $R^2=0.9923$ at -0.29V. For the silver electrode the LoD ranged from 16 $\mu\text{g/ml}$ at pH=10 to 0.9 $\mu\text{g/ml}$ at pH=5 and pH=11, respectively.

The average Coefficient of Variation also followed the trend observed for gold electrodes showing a higher precision of -3.90% and -1.61% at pH=5 and 11, respectively.

Principal Component Analysis of the different digoxin solutions were also performed for silver electrodes, as shown in Figure 8. The PCA analyses showed a similar behaviour to that observed in gold at pH=11 and showed a better clustering than other PHs. Hence, the best possible analytical conditions for the analysis of digoxin on a silver electrode should be conducted at pH=11. Also, the variability achieved in the analysis of the PCA plot for figure 8 was PC1(53.71%) and PC2(22.91%).

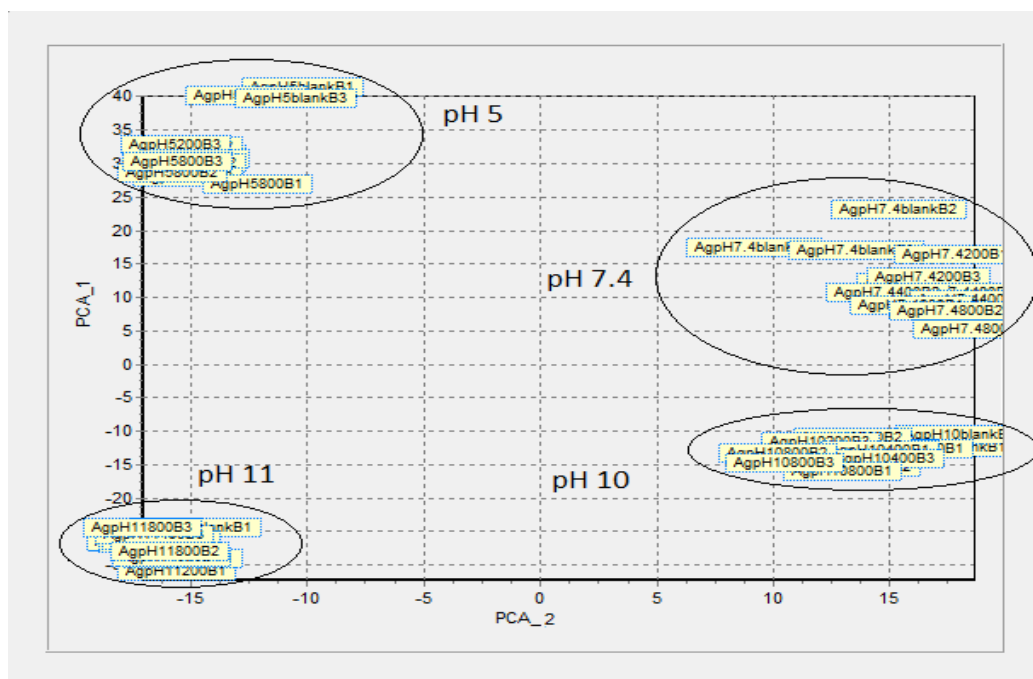


Figure 8. PCA scatterplot of Silver electrode at different pHs. of 5, 7.4, 10, 11. Percentage of variability: PC1=51.30%; PC2=29.94%.

4. CONCLUSIONS

The results obtained by studying digoxin with Ag and Au electrodes in solution at different pHs showed that both electrodes are suitable for the analytical determination of digoxin in solution in the range of concentrations from 3.92 to 14.81 µg/ml.

Using a gold electrode, the best analytical conditions, given by the LoD and the linearity of the calibration curve, showed that the alkaline environment at pH11 is the ideal one. For this the LoD was 1.7 µg/ml, with a corresponding coefficient of variance of 2.07% and 4.13% at pH 11 for both RED-OX and OX-RED sweeps, respectively.

Silver electrodes showed the best LoD (0.9 µg/ml) at pH5 and at pH11. The results obtained characterised by a coefficient of variation of -3.90% and -1.61% at pH5 and 11, respectively.

The metal electrodes studied seem to be good candidates in the analysis of digoxin via cyclic voltammetry replacing the mercury one and being able to quantify trace of this alkaloid in the range in optimum alkaline solutions at pH11. It is also important to emphasize the role that the surface oxides may play in digoxin redox behaviour and the catalytic influence in the electrochemical behaviour of this molecule in solid electrodes.

References

1. G. Paniagua González, P. Fernández Hernando, J. S. Durand Alegría, *Anal. Chim. Acta*, 638(2009) 209–212
2. H. Kinoshita, T. Taniguchia, M. Nishiguchia, H. Ouchia, T. Minamia, T. Utsumib, H. Motomurac, T. Tsudaa, T. Ohtaa, S. Aokia, M. Komadaa, T. Kamamotoa, A. Kubotad, C. Fukee, T. Araoe, T. Miyazakie, S. Hishida, *Forensic. Sci. Int.*, 133(2003) 107–112
3. M. Yao, H. Zhang, S. Chong, M. Zhu, R. A. Morrison, *J. Pharm. Biomed. Anal.*, 32 (2003) 1189–1197
4. S. A. Jortani, A. Pinar, N. A. Johnson, R. Valdes Jr, *Clin. Chim. Acta*, 283(1999) 159–169
5. M. A. Pullen, M. R. Harpel, T. M. Danoff, D. P. Brooks, *J. Immunol. Methods.*, 336(2008) 235–241
6. G. Paniagua González, P. Fernández Hernando, J.S. Durand Alegría, *Biosens. Bioelectron.*, 23(2008) 1754–1758
7. P. H. Cobb, *Analyst*, 101(1976) 768–776
8. F. Pellati, R. Brunib, M. G. Bellardi, A. Bertaccini, S. Benvenuti, *J. Chromatogr. A*, 1216(2009) 3260–3269
9. W. N. Moore, L. T. Taylor, *J. Nat. Prod.* 59(1996) 690–693
10. A. Jedlic`ka, T. Grafnetterova, V. Miller, *J. Pharm. Biomed. Anal.*, 33(2003) 109–115
11. M.-C. Tzou, R.A. Sams, R.H. Reuning, *J. Pharm. Biomed. Anal.*, 13(1995) 1531–1540
12. K. L. Kelly, B. A. Kimball, J. J. Johnston, *J. Chromatogr. A*, 711 (1995) 289–295
13. E. Hershenhart, R. L. McCreery, R. D. Knight, *Anal. Chem.*, 56(1984) 2256–2257
14. Y. Hashimoto, K. Shibakawa, S. Nakade, Y. Miyata, *J. Chromatogr. B*, 869(2008) 126–132
15. F. Guan, A. Ishii, H. Seno, K. Watanabe-Suzuki, T. Kumazawa, O. Suzuki, *Anal. Chem.*, 71(1999) 4034–4043
16. Y. Gaillard, G. Pepin, *J. Chromatogr. B*, 733(1999) 181–229
17. S. Li, G. Liu, J. Jia, Y. Miao, S. Gu, P. Miao, X. Shi, Y. Wang, C. Yu, *Clin. Biochem.*, 43(2010) 307–313
18. J. Smalley, A. M. Marino, B. Xin, T. Olah, P. V. Balimane, *J. Chromatogr. B*, 854(2007) 260–267
19. J. Wang, J. S. Mahmoud, P. A. M. Fariast, *Analyst*, 110(1985) 855–859
20. E. A. Ivanovskaya, Y. V. Bobleva, R. S. Karpov, *J. Anal. Chem.*, 55-11(2000) 1077–1079
21. H. Qi, C. Zhang, *Anal. Chim. Acta*, 501(2004) 31–35
22. Y. Ikeda, Y. Fujii, M. Umemura, T. Hatakeyama, M. Morita, M. Yamazaki, *J. Chromatogr. A*, 746(1996) 255–260
23. Q. Wan, X. Chris Le, *J. Chromatogr. B*, 734(1999) 31–38
24. M. Pasta, F. La Mantia, Y. Cui, *Electroch. Acta* 55 (2010) 5561–5568
25. D.W. Kirk, F.R. Foulkes, W.F. Graydon, *J. Electrochem. Soc.* 127 (1980) 1069
26. H. H. Hassan, M. A. M. Ibrahim, S. S. Abd El Rehim, M. A. Amin, *Int. J. Electrochem. Sci.*, 5 (2010) 278 - 294
27. B. Uslu, S. A. Ozkan, *Comb. Chem. & High Throughput Screen*, 10(2007) 495–513
28. W. Wei, X. Mao, L. Ortiza, D. Sadoway, *J. Mater. Chem.*, 21(2011) 432–438

29. S. Atkins, J.M. Sevilla, M. Blazquez, T. Pineda, R. Jimenez-Perez, J. Gonzalez-Rodriguez, *Int J. Electrochem Sci*, 8 (2013) 2056-2068.
30. S. Atkins, J.M. Sevilla, M. Blazquez, T. Pineda, J. Gonzalez-Rodriguez, *Electroanalysis*, 22 (2010) 2961-2966.
31. R. Jiménez-Pérez, J.M. Sevilla, T. Pineda, M. Blázquez, J. Gonzalez-Rodriguez, *J. Electroanal. Chem.* 766 (2016) 141–146
32. R. Jiménez-Pérez, J.M. Sevilla, T. Pineda, M. Blázquez, J. Gonzalez-Rodriguez, *Electrochimica Acta* 193 (2016) 154–159
33. A. F. Belchior Andrade, S. K. Mamo, J. Gonzalez-Rodriguez, *Anal. Chem.*, 89 (2017) 445–1452.
34. R. Jiménez-Pérez, J.M. Sevilla, T. Pineda, M. Blázquez, J. Gonzalez-Rodriguez, *Int. J. Electrochem. Sci.*, 11 (2016) 10473 – 10487.
35. R. Jiménez-Pérez, J.M. Sevilla, T. Pineda, M. Blázquez, J. Gonzalez-Rodriguez, *Electrochimica Acta*, 111 (2013) 601-607
36. M.J. Nicol, *Gold Bull.*, 13(1980)105-111.

© 2017 The Authors. Published by ESG (www.electrochemsci.org). This article is an open access article distributed under the terms and conditions of the Creative Commons Attribution license (<http://creativecommons.org/licenses/by/4.0/>).